INSTITUT PASTEUR

Research in Microbiology 161 (2010) 876–882

www.elsevier.com/locate/resmic

Cloning and characterization of a *p*-cymene monooxygenase from *Pseudomonas chlororaphis* subsp. *aureofaciens*

Tapan K. Dutta [a,b,*], Joydeep Chakraborty [a], Madhumita Roy [a], Debajyoti Ghosal [a], Pratick Khara [a], Irwin C. Gunsalus [b,1]

[a] *Department of Microbiology, Bose Institute, P-1/12 CIT Scheme VIIM, Kolkata 700054, India*
[b] *NHEERL, Gulf Ecology Division, U.S. EPA, Gulf Breeze, FL 32561-5299, USA*

Received 31 May 2010; accepted 5 September 2010
Available online 28 October 2010

Abstract

p-Cymene monooxygenase is the enzyme system that catalyzes the hydroxylation of *p*-cymene to 4-isopropylbenzyl alcohol (*p*-cumic alcohol), the initial step in the assimilation of *p*-cymene by *Pseudomonas chlororaphis* subsp. *aureofaciens*. Cloning and sequencing of single NADH-dependent cytochrome c reductase gene (*cymA*) present in *P. chlororaphis* subsp. *aureofaciens* was described earlier. In this study, analysis of the upstream sequence of *cymA* revealed two open reading frames, designated as *cymB* (495 bp) and *cymM* (1128 bp). Database searches with the *cymM* gene product showed similarity to integral-membrane di-iron enzymes, while that with *cymB* showed no significant similarity to other known proteins with the exception of epoxystyrene isomerases. Expression of all three components (*cymMBA*) in *Escherichia coli* confirmed its ability for *p*-cymene methyl group hydroxylation, while expression of *cymM* and *cymA* along with the partially truncated *cymB* gene showed an 85% decrease in the hydroxylation capacity. Our results suggest for the first time that the small protein, CymB, having no conserved domains in protein databases, is involved as enhancer/activator in *p*-cymene hydroxylation.

Keywords: *p*-Cymene; Methyl hydroxylase; Monooxygenase; Non-heme di-iron enzyme; *Pseudomonas*

1. Introduction

Biogeochemical reserves and industrial activities are the major sources of alkylated aromatic compounds which form an important group of environmental pollutants or their precursors in the ecosystem (Dutta, 2005; Radke, 1987). Microorganisms that mineralize a variety of methyl aromatic compounds have been isolated and their metabolism via side-chain hydroxylation has been well documented (Assinder and Williams, 1990; Defrank and Ribbons, 1977; Dutta et al., 1998; Hopper, 1988). However, the oxygenase system that hydroxylates methyl substituents of the aromatic ring, the catalytic iron center and the reaction cycle largely remains to be defined. Catalytic centers, which contain iron prosthetic groups, have been well documented for several oxygenases. The most abundant center is a unique heme-thiolate monooxygenase which contains more than 500 related protein sequences (Nelson, 2006). A few other well-studied oxygen reaction centers are the $Fe_2(\mu O)_2$ cluster, found in methane monooxygenase, alkane hydroxylase and other non-heme di-iron enzymes (Fox et al., 1988; Schwartz et al., 2008; Shanklin et al., 1994, 2009; Shanklin and Whittle, 2003) and dissociable ferrous, mononuclear non-heme iron coordination sites (Kovaleva and Lipscomb, 2008).

To understand the structural aspect and the mechanistic details, we selected *p*-cymene, an aromatic-terpenoid of biosynthetic origin, as the representative model for alkylated aromatics. *p*-Cymene is a natural aromatic hydrocarbon which occurs in the oils of many gymnospermic and angiospermic

* Corresponding author. Department of Microbiology, Bose Institute, P-1/12 CIT Scheme VIIM, Kolkata 700054, India. Tel.: +91 33 2569 3241; fax: +91 33 2355 3886.
E-mail address: tapan@bic.boseinst.ernet.in (T.K. Dutta).
[1] Professor Irwin C. Gunsalus passed away October 25, 2008.

0923-2508/$ - see front matter © 2010 Institut Pasteur. Published by Elsevier Masson SAS. All rights reserved.
doi:10.1016/j.resmic.2010.10.008

plants (Benchaar et al., 2008; Singh et al., 1999). Moreover, it has been observed as the dead-end product in anaerobic enrichment cultures of certain non-aromatic monoterpenes (Harder and Probian, 1995).

Oxidative catabolism of *p*-cymene had been studied widely and the assimilating pathway was already established (Defrank and Ribbons, 1977; Eaton, 1997; Lee et al., 2006; Madhyastha et al., 1968). The upper pathway of *p*-cymene metabolism occurs by progressive oxidation of the methyl side-chain to carboxylic acid. Cloning and characterization of the *cym* operon, which was reported to be involved in the conversion of *p*-cymene to *p*-cumate in *Pseudomonas putida* F1 revealed the presence of a two-component methyl monooxygenase (Eaton, 1997). Similar oxidation of methyl groups was reported for toluene and *m*- and *p*-xylenes (Assinder and Williams, 1990; Harayama et al., 1989, 1992). For example, xylene monooxygenase, a two-component system in *P. putida* mt-2, is biochemically most closely related to *p*-cymene monooxygenase, and its terminal component, XylM, carries similarity with *n*-alkane hydroxylase and steroyl-CoA desaturase terminal components (Kok et al., 1989; Shanklin et al., 1994; Suzuki et al., 1991). On the other hand, the flavoprotein reductase, XylA differs from the corresponding alkane and, in part, from desaturase proteins.

The reductase sequence of *p*-cymene monooxygenase from *Pseudomonas aureofaciens* reclassified as *Pseudomonas chlororaphis* subsp. *aureofaciens* (Peix et al., 2007) was reported in our previous communication (Dutta and Gunsalus, 1997). Moreover, its high similarity with various oxygenase-coupled flavoproteins of both prokaryotic and eukaryotic origin including systems of heme and non-heme monooxygenases, aromatic dioxygenaes and reductases involved in other biological functions had also been demonstrated. The present study reports the genetic characterization and expression of the three-component *p*-cymene monooxygenase, including a small open reading frame, *cymB*, involved in *p*-cymene methyl hydroxylation.

2. Materials and methods

2.1. Organism, culture conditions and plasmid

P. chlororaphis subsp. *aureofaciens* strain PJC was cultured in PAS medium (Gunsalus and Wagner, 1978) with *p*-cymene (1 g l^{-1}) as the sole source of carbon and energy as described earlier (Dutta and Gunsalus, 1997). Recombinant strain *Escherichia coli* JM109 (Yanisch-Perron et al., 1985) was grown in Luria-Bertani (LB) medium (Davis et al., 1980) overnight at 37 °C. Bacto agar (1.5%), Difco Laboratories, Detroit, MI was added for solid media.

2.2. Cloning and DNA manipulation of the p-cymene monooxygenase genes

The N-terminal amino acid sequence and the near C-terminal conserved sequences of related iron-sulfur flavoproteins associated with aromatic methyl hydroxylase and ring-hydroxylating monooxygenases were used to design primers for PCR processing (Dutta and Gunsalus, 1997). The PCR product used as a probe in southern and colony hybridization for the 8 kb (*Bgl*II fragment) clone of the total cell DNA in pLV59 (O'Connor and Humphries, 1982) has been described previously (Dutta and Gunsalus, 1997). The 8 kb insert in pLV59 (pTD101) was digested with *Hin*dIII and *Kpn*I, gel-purified and inserted into the *Hin*dIII and *Kpn*I unique sites within the *lacZ*α gene of the plasmid pBluescriptII SK (Fig. 1). The recombinant plasmid (pTD102) was transformed in *E. coli* on selective medium containing ampicillin (100 μg ml^{-1}), IPTG (0.25 mM) and X-gal (0.02%). White colonies were picked for further analysis. To delete the *Hin*dIII-*Bgl*II region which is from plasmid pLV59 and to delete the *Pst*I site from the pBluescriptII SK, the recombinant plasmid was digested with *Bgl*II and *Spe*I (*Spe*I is one of the multiple cloning sites of pBluescriptII SK). The overhangs were filled by the action of Klenow fragment of DNA polymerase I, ligated with T4 DNA ligase and transformed into *E. coli* under similar selection pressure. The white colonies carrying the *Bgl*II-*Kpn*I region of the original 8 kb insert in pBluescriptII SK (pTD103, Fig. 1) which essentially lost the *Bgl*II and *Spe*I sites due to Klenow filling, was further digested with *Hin*cII and *Pst*I to delete a fragment (123 bp, nucleotide 1599 to 1721) from the *cymB* gene. *Hin*cII produced the blunt end but the 3′ overhang from *Pst*I was repaired by the 3′→5′ exonuclease activity of T4 DNA polymerase incubated in the presence of all four dNTPs, ligated (pTD104, Fig. 1) and transformed into *E. coli*. The variants containing different inserts were confirmed by restriction analysis of the respective plasmids and DNA sequencing analysis.

2.3. DNA sequencing and analysis

DNA sequences were determined by the dideoxy chain termination method using double-stranded DNA as the template (Sanger et al., 1977). Sequencing was accomplished according to the manufacturer's specifications for *Taq* DNA polymerase-initiated cycle sequencing reactions using fluorescently labeled di-deoxynucleotide terminators and primers on an Applied Biosystem Model 373A DNA sequencer. (Perkin–Elmer Applied Biosystems, Inc.). Sequence data were aligned and edited using DNASTAR (DNASTAR Inc., Madison, WI, USA). Searches for specific nucleotide or amino acid sequences in databases were carried out with the BLAST program (Altschul et al., 1990), while ClustalX v1.81 (Thompson et al., 1997) was used to obtain multiple sequence alignments for protein sequences.

2.4. Expression of recombinant strains and metabolite analysis

Recombinant strains were grown in LB medium at 37 °C, supplemented with ampicillin (100 μg ml^{-1}). After 2 h incubation, inducer, IPTG was added to a final concentration of 1 mM. Induction proceeded for 3 h at 37 °C and then cells were collected by centrifugation, washed twice using

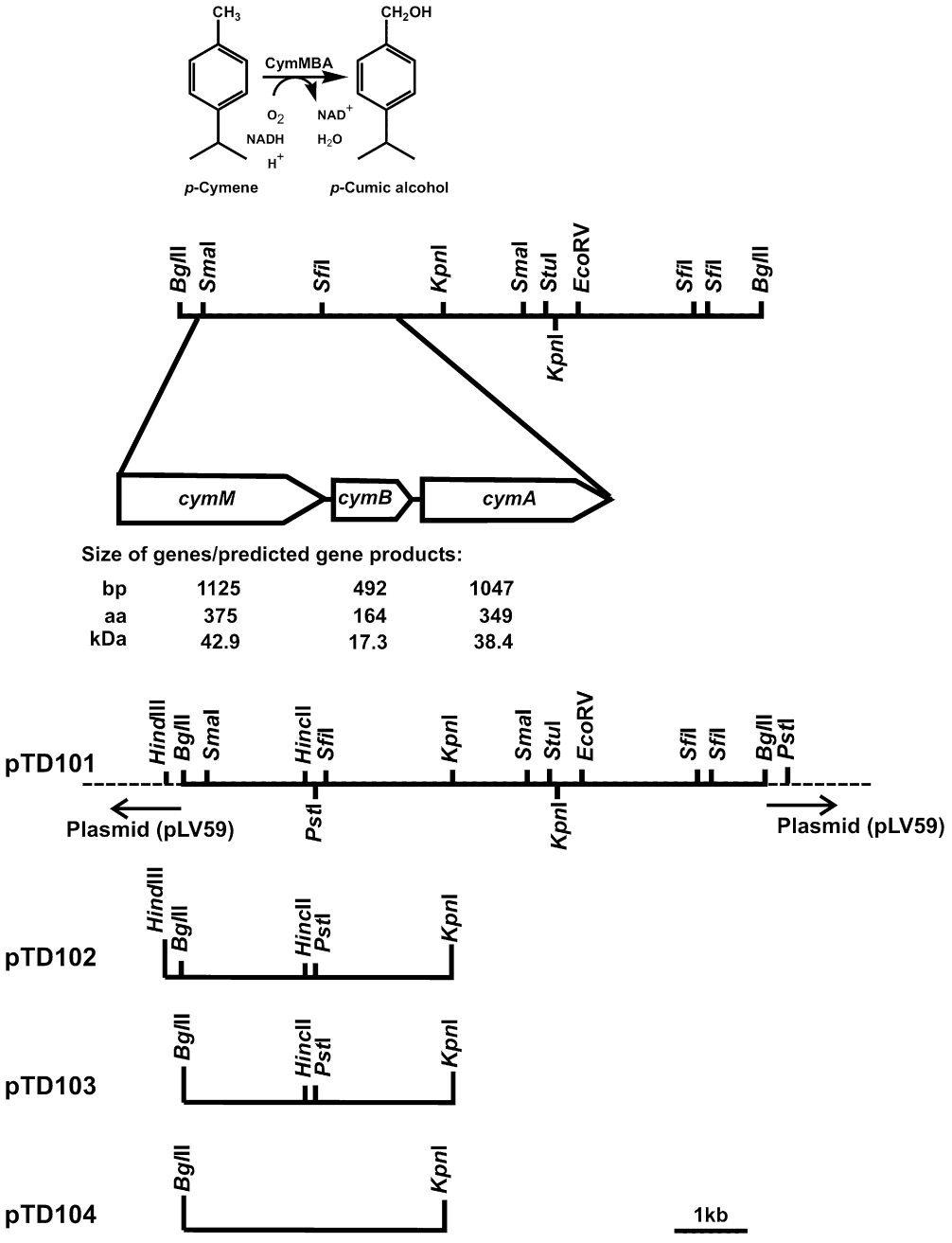

Fig. 1. Proposed reaction sequence for the catabolism of *p*-cymene mediated by the enzymes encoded in the *Bgl*II-*Kpn*I fragment (pTD103) and partial restriction map of the 8 kb *Bgl*II genomic fragment of *P. chlororaphis* subsp. *aureofaciens* containing the *cymM*, *cymB* and *cymA* genes in plasmid pLV59 and subcloned fragments in plasmid pBluescriptII SK.

potassium phosphate buffer (50 mM, pH 7.0) and resuspended in the same buffer at an OD_{600} of 2.0. The cell suspensions (20 ml) were each incubated in 100 ml flasks in the presence of 5 mM *p*-cymene and *p*-cumic alcohol individually for 18 h at 30 °C under constant shaking. Each experiment was carried out in triplicate. Cells were removed by centrifugation and the supernatant was acidified to pH 2.0 using concentrated hydrochloric acid and then extracted thrice with an equal volume of ethyl acetate. The combined extracts were dried over anhydrous sodium sulfate and evaporated under reduced pressure. An *E. coli* strain without the plasmid was used as a control. The rate of transformation of substrate was expressed as *n*moles of substrate transformed (analyzed by HPLC) per μg of cell dry weight (CDW) per hour.

Metabolites were analyzed by reverse phase high performance liquid chromatography (HPLC) instrument equipped with a diode array detector and/or by gas chromatography-mass spectrometry (GC–MS) with a Hewlett–Packard 5890 series II gas chromatograph equipped with HP5971 mass-selective and HP 5965B infrared detectors. The ethyl acetate extract of resting cell culture was injected onto the HPLC C_{18} column system and then eluted with acetonitrile-water (65:35)

for 20 min, and the metabolites were detected at 254 nm. The identity of the metabolites was confirmed from comparison of retention time and UV spectrum with authentic samples. In GC–MS analysis, metabolites were separated on a type HP-5 capillary column (25 m × 0.32 mm, 0.25 μm film thickness) with helium as the carrier gas (23 cm/s). The column temperature was kept isothermally at 50 °C for 1 min and then increased to 290 °C at a rate of 5 °C min^{-1}. The mass spectrometer was operated at electron ionization energy of 70 eV. Injector, transfer line and analyzer temperatures were set at 150 °C, 300 °C and 300 °C, respectively. Instrumental library searches and comparisons with authentic compounds were used for the identification of metabolites. The relative amounts of metabolites were calculated from the peak areas of GC–MS total ion current chromatograms. The total ion current integrated responses excluding the peak area of the residual substrate were used as 100% internal standard values for each sample analyzed. Parallel processes without substrate were also included.

2.5. Accession number

The nucleotide sequence described in this report has been deposited with GenBank under the accession number AF012555.

3. Results and discussion

3.1. Nucleotide sequence of cymM and cymB

The physical map of the *Bgl*II fragment containing genes encoding multi-component *p*-cymene monooxygenase is shown in Fig. 1. We determined the sequence of a 1759 bp region upstream to *cymA* sequence. Computational analysis of the sequence showed the presence of two open reading frames, designated as *cymM* and *cymB*. The start codon of each open reading frame was preceded by a potential ribosomal binding site, suggesting that each open reading frame could be translated. The first open reading frame *cymM* extending from nucleotide 97 to 1224 could encode a protein of 375 amino acids (with estimated molecular mass of 42.9 kDa). The second open reading frame extending from 1240 to 1734 could encode a protein of 164 amino acids (with estimated molecular mass 17.3 kDa).

3.2. Sequence comparisons

A search for proteins related to CymM revealed that it has 81.6% identity in 376 amino acid residues to CymAa, the oxygenase component of *p*-cymene monooxygenase from *P. putida* F1 (Eaton, 1997); 74.7% (in 368 amino acid residues) to CymAa, putative oxygenase component of *p*-cymene monooxygenase from *Burkholderia xenovoran* LB400 (Chain et al., 2006); 37.2% (in 363 amino acid residues) to XylM, oxygenase component of xylene monooxygenase from *P. putida* (Suzuki et al., 1991); 35.8% (in 363 amino acid residues) to NtnMA, monooxygenase component of 4-nitrotoluene hydroxylase from *Pseudomonas* sp. strain TW3 (James and Williams, 1998) and 24.8% (in 278 amino acid residues) to AlkB, terminal component of alkane hydroxylase from *Pseudomonas oleovorans* (Kok et al., 1989). CymM also showed similarity to a number of other xylene monooxygenase components, terminal components of alkane hydroxylases and fatty acid desaturases in the database, which were either biochemically characterized or annotated as putative sequences from complete genome or plasmid analyses. The amino acid sequence alignment of CymM, CymAa (strain LB400), CymAa (strain F1), XylM, NtnMA and AlkB is shown in Fig. 2A. Among the sequences, some 40 amino acids including 10 histidines were found to be conserved. Conserved histidine residues present in non-heme integral membrane desaturases and hydroxylases which are proposed to be the binding motif for catalytic iron center (Shanklin et al., 1994) are also distinct in CymM in the motif of $HX_3HX_{25}HX_3HHX_{133}HX_2HH$ (Fig. 2A). Site-directed mutagenic studies have shown that these eight histidine residues are essential for catalysis in rat desaturase (Shanklin et al., 1994). Mossbauer studies on AlkB demonstrated evidence for the di-iron cluster in the integral membrane enzyme (Shanklin et al., 1997). However, the other di-iron centers present in soluble enzymes and used for oxygen activation are distinct from the integral membrane enzyme in consensus motif (Fox et al., 1988; Gallagher et al., 1998; Shu et al., 1997).

A database search of CymB showed 67.5% identity in 157 amino acid residues with the hypothetical protein, Bxe_A3560 (167 amino acids) from *Burkholderia xenovorans* LB400 (Chain et al., 2006) apart from the styrene isomerase (StyC). StyC is responsible for isomerization of epoxystyrene into phenylacetaldehyde in the catabolic pathway of styrene from *Pseudomonas fluorescens* ST (Beltrametti et al., 1997). It is a protein of 169 amino acids and has 41% identity and more than 70% similarity to CymB. Other well characterized epoxystyrene isomerases, StdC and StyC reported from *Pseudomonas* sp. strain VLB120 (Panke et al., 1998) and *Pseudomonas* sp. strain Y2 (Velasco et al., 1998), respectively, are very similar (92% identity) to StyC from *P. fluorescens* ST. Amino acid sequence alignment of CymB, hypothetical protein (Bxe_A3560) from strain LB400, StdC from strain VLB120 and StyC from strains ST and Y2 is shown in Fig. 2B. Although 30 amino acids were observed to be conserved among these sequences, database searches with CymB did not show the presence of any motif for prosthetic center or known conserved domain. Thus, sequence comparison as such was unable to predict any functional importance. The pairwise sequence identity of CymB with other eposystyrene isomerases is in the range of 39–43%, in contrast to 92% identity amongst the well characterized eposystyrene isomerases, indicating that CymB is either a distant homolog of eposystyrene isomerases or has another unknown function. However, no epoxystyrene isomerase activity was observed with either the whole cell or cell-free extract of *P. chlororaphis* subsp. *aureofaciens* or recombinant *E. coli* carrying pTD103 (discussed in later section), suggesting the possible role of CymB either in *p*-cymene hydroxylation or in subsequent metabolic degradation.

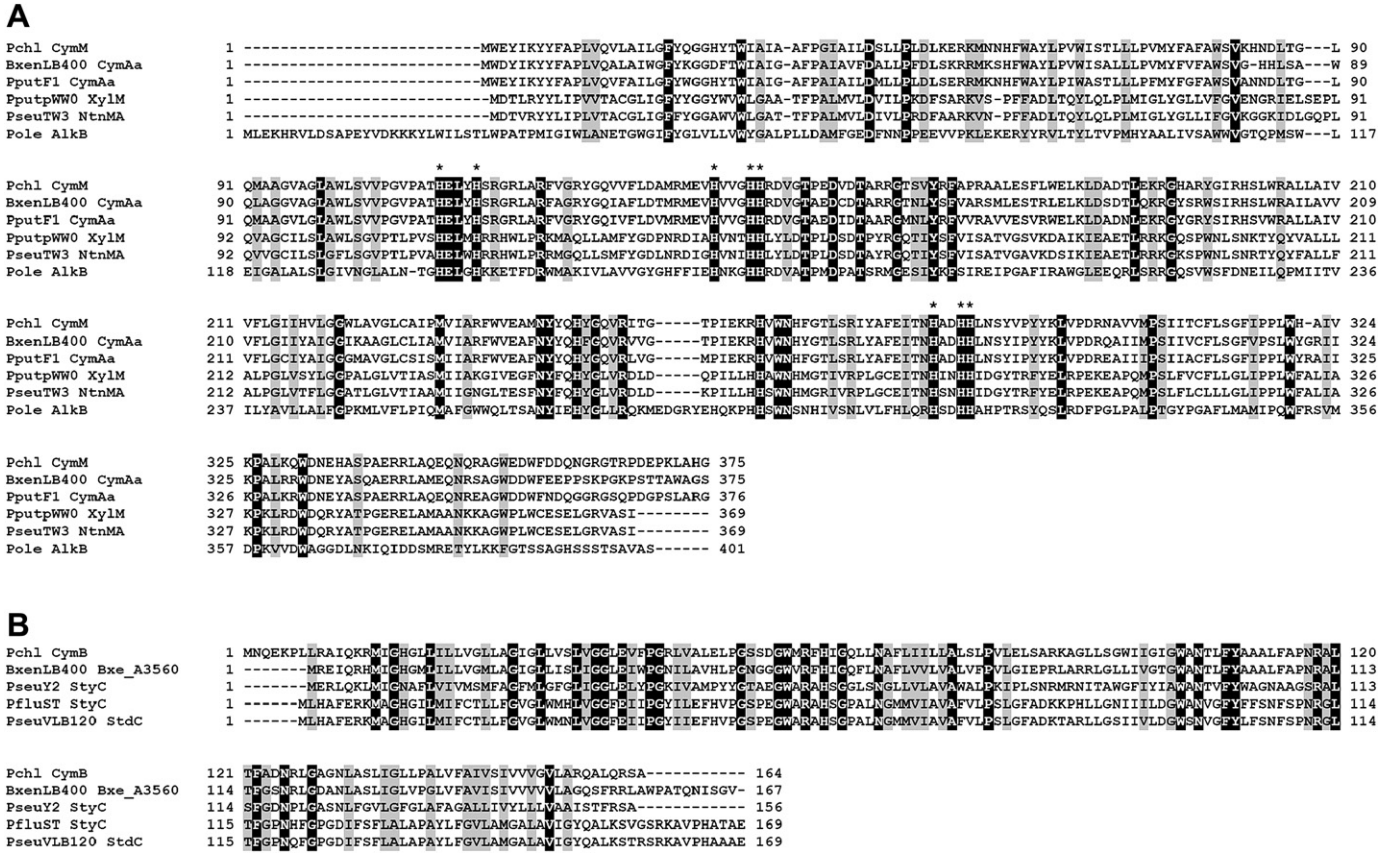

Fig. 2. Alignment of the amino acid sequences of CymM, CymAa (strain LB400), CymAa (strain F1), XylM, NtnM, and AlkB (A) and that of CymB, Bxe_A3560 (strain LB400), StyC (strain ST), StyC (strain Y2), and StdC (B). Identical and similar amino acid residues among aligned sequences are shaded in back and gray, respectively. Dashes indicate gaps. Eight conserved histidine residues proposed to be the binding motif for the catalytic iron center (Shanklin et al., 1994) are indicated by asterisks (A). In both the panels (A and B), protein names are preceded by the abbreviated names of the respective source organism. Pchl, *Pseudomonas chlororaphis* subsp. *aureofaciens*; BxenLB400, *Burkholderia xenovoran* LB400; PputF1, *Pseudomonas putida* F1; PputpWW0, *Pseudomonas putida* TOL plasmid pWW0; PseuTW3, *Pseudomonas* sp. strain TW3; Pole, *Pseudomonas oleovorans*; PseuY2, *Pseudomonas* sp. strain Y2; PfluST, *Pseudomonas fluorescens* ST and PseuVLB120, *Pseudomonas* sp. strain VLB120.

It is worthwhile mentioning that the complete genome analysis of *B. xenovorans* LB400 indicated the presence of putative sequences for *p*-cymene methyl hydroxylase (Chain et al., 2006). The putative terminal oxygenase and reductase components from strain LB400 are 74.7 and 77% (in 348 amino acid residues) identical to CymM and CymA from *P. chlororaphis* subsp. *aureofaciens*, while the hypothetical protein (Bxe_A3560) from strain LB400 has 67.5% identity with CymB. Although there is no functional evidence, these three putative proteins in strain LB400 maintain the gene order as that of *cymMBA*, suggesting a similar *p*-cymene hydroxylation system as that of the *p*-cymene monooxygenase from *P. chlororaphis* subsp. *aureofaciens*.

3.3. Expression of p*-cymene monooxygenase and the role of CymB*

Recombinant *E. coli* JM109 (pTD103) containing part of the 8 kb fragment from *P. chlororaphis* subsp. *aureofaciens* containing *cymM*, *cymB* and *cymA* was found to transform *p*-cymene to *p*-cumic alcohol and *p*-cumic aldehyde. Transformation of *p*-cymene to *p*-cumic alcohol and *p*-cumic aldehyde was also observed with the recombinant strain containing pTD104 where the 123 bp (1599–1721) from *cymB* had been deleted (Fig. 1). In contrast, the strain, *E. coli* JM109 without pTD103 or pTD104 was found to be unable to catabolize *p*-cymene. Biotransformation of *p*-cymene to *p*-cumic aldehyde by methyl hydroxlase is due to the monooxygenation of *p*-cumic alcohol with the formation of *gem*-diol (α,α'-dihydroxy *p*-cymene) followed by spontaneous dehydration. This has been verified from reaction product(s) obtained from *p*-cumic alcohol used as substrate. Previous studies on xylene monooxygenase and *p*-cymene monooxygenase also described a similar event with the formation of the corresponding aldehyde (Eaton, 1997; Harayama et al., 1986). Formation of *p*-cumic acid is believed to be generated from *p*-cumic aldehyde by non-enzymatic transformation as described earlier (Eaton, 1997). This has been supported by the evidence from the incubation of *p*-cumic aldehyde with non-inoculated medium. Apart from the involvement of *p*-cymene monooxygenase in the transformation of *p*-cumic alcohol to *p*-cumic aldehyde and the non-enzymatic transformation of *p*-cumic aldehyde to *p*-cumic acid, *P. chlororaphis* subsp. *aureofaciens* does harbor *p*-cumic alcohol

dehydrogenase and *p*-cumic aldehyde dehydrogenase similar to the metabolic pathways of other methylated aromatic compounds (Eaton, 1997; Harayama et al., 1986). The presence of these dehydrogenases was ascertained from the higher transformation rates of the respective substrates by *P. chloroaphis* subsp. *aureofaciens* both under in vivo and in vitro conditions in comparison to that obtained from recombinant *E. coli* containing pTD103 or non-enzymatic incubation. The identity of various metabolites and non-enzymatically transformed products was ascertained from HPLC analysis by comparing the retention time, co-elution profile and UV–visible spectrum (recorded by diode array detector) of the individual metabolite/product with those of the authentic compounds analyzed under identical conditions. The catalytic efficiency in the partially deleted *cymB* (pTD104) transformant decreased significantly in comparison to that of pTD103 where the full length three-component system was present.

The GC–MS data of the biotransformation products also showed a characteristic mass fragmentation pattern for *p*-cumic alcohol (GC $R_t = 16.11$ min; MS *m/z* [%]: 150 [M^+] [47], 135 [100], 119 [32], 107 [39], 105 [46], 91[30], 79 [37], 77 [20]), *p*-cumic aldehyde (GC $R_t = 14.86$ min; MS *m/z* [%]: 148 [M^+] [68], 133 [100], 119 [29], 105 [69], 91[22], 79 [21], 77 [29]), and *p*-cumic acid (GC $R_t = 19.62$ min; MS *m/z* [%]: 164 [M^+] [45], 149 [100], 131 [15], 119 [32], 105 [33], 91 [13], 79 [14], 77 [19]). HPLC data revealed that the recombinant *E. coli* containing pTD103 produced 61, 12.5 and 26.5% of *p*-cumic alcohol, *p*-cumic aldehyde and *p*-cumic acid respectively. While from pTD104, the total amount (sum of peak areas representing *p*-cumic alcohol, *p*-cumic aldehyde and *p*-cumic acid) was 14.7% relative to the total products obtained from pTD103. The relative ratio of products with pTD104 was 73.5, 8.2 and 18.3% respectively. These values represent averages from three determinations with standard errors in the range of ±2–7%. On the other hand, the rate of transformation of *p*-cymene by the recombinant *E. coli* strains carrying plasmids pTD103 and pTD104 was found to be 7.6 and 1.1 *n* moles (μg CDW)$^{-1}$ h^{-1} respectively. Therefore, it appears that CymB has some role in enhancing hydroxylation of *p*-cymene. It is important here to mention that a number of multi-component hydroxylating systems including methane, toluene and alkene monooxygenases and phenol hydroxylases have been reported where one or the other components do not contain any binding motif but are supposed to be effector proteins in catalysis (Schwartz et al., 2008 and references there in). Currently, the best characterized system is three-component methane monooxygenase, where the MMOB component does not have any prosthetic group binding motif but has been characterized as the effector protein. This was shown to increase the rate and yield of multiple turnovers, to affect spectral properties of the di-iron center, product profile and redox potential and also to change the conformation of diferric hydroxylase (Davydov et al., 1997; Fox et al., 1991). The significant difference in the turnover of oxygenated product(s) from *p*-cymene in the presence of full length CymB and deleted CymB, as reported in this study, is an important first step to understanding the exact role of CymB in the reaction cycle.

Acknowledgments

This manuscript is dedicated to the memory of I. C. Gunsalus (Gunny). The authors wish to express appreciation to Professor K. P. Das and Dr. Geoffrey Mattison for reviewing the manuscript. This work was supported in part by a National Research Council Research Associate Award, USA (T.K.D.) and Bose Institute, Kolkata, India.

References

Altschul, S.F., Gish, W., Miller, W., Myers, E.W., Lipman, D.J., 1990. Basic local alignment search tool. J. Mol. Biol. 215, 403–410.

Assinder, S.J., Williams, P.A., 1990. The TOL plasmids: determinants of the catabolism of toluene and xylenes. Adv. Microb. Physiol. 31, 1–69.

Beltrametti, F., Marconi, A.M., Bestetti, G., Colombo, C., Galli, E., Ruzzi, M., Zennaro, E., 1997. Sequencing and functional analysis of styrene catabolism genes from *Pseudomonas fluorescens* ST. Appl. Environ. Microbiol. 63, 2232–2239.

Benchaar, C., Calsamiglia, S., Chaves, A.V., Fraser, G.R., Colombatto, D., McAllister, T.A., Beauchemin, K.A., 2008. A review of plant-derived essential oils in ruminant nutrition and production. Anim. Feed Sci. Technol. 145, 209–228.

Chain, P.S., Denef, V.J., Konstantinidis, K.T., et al., 2006. *Burkholderia xenovorans* LB400 harbors a multi-replicon, 9.73-Mbp genome shaped for versatility. Proc. Natl. Acad. Sci. USA 103, 15280–15287.

Davis, R.W., Botstein, D., Roth, J.R., 1980. Advanced Bacterial Genetics. Cold Spring Harbor Laboratory. Cold Spring Harbor, N.Y.

Davydov, A., Davydov, R., Graslund, A., Lipscomb, J.D., Andersson, K.K., 1997. Radiolytic reduction of methane monooxygenase dinuclear iron cluster at 77 K. EPR evidence for conformational change upon reduction or binding of component B to the diferric state. J. Biol. Chem. 272, 7022–7026.

Defrank, J.J., Ribbons, D.W., 1977. *p*-Cymene pathway in *Pseudomonas putida*: initial reactions. J. Bacteriol. 129, 1356–1364.

Dutta, T.K., 2005. Origin, occurrence, and biodegradation of long-side-chain alkyl compounds in the environment: a review. Environ. Geochem. Health 27, 271–284.

Dutta, T.K., Gunsalus, I.C., 1997. Reductase gene and protein structures: *p*-cymene methyl hydroxylase. Biochem. Biophys. Res. Commun. 233, 502–506.

Dutta, T.K., Selifonov, S.A., Gunsalus, I.C., 1998. Oxidation of methyl-substituted naphthalenes: pathways in a versatile *Sphingomonas paucimobilis* strain. Appl. Environ. Microbiol. 64, 1884–1889.

Eaton, R.W., 1997. *p*-Cymene catabolic pathway in *Pseudomonas putida* F1: cloning and characterization of DNA encoding conversion of *p*-cymene to *p*-cumate. J. Bacteriol. 179, 3171–3180.

Fox, B.G., Surerus, K.K., Munck, E., Lipscomb, J.D., 1988. Evidence for a μ-oxo-bridged binuclear iron cluster in the hydroxylase component of methane monooxygenase, Mössbauer and EPR studies. J. Biol. Chem. 263, 10553–10556.

Fox, B.G., Liu, Y., Dege, J.E., Lipscomb, J.D., 1991. Complex formation between the protein components of methane monooxygenase from *Methylosinus trichosporium* OB3b. Identification of sites of component interaction. J. Biol. Chem. 266, 540–550.

Gallagher, S.C., George, A., Dalton, H., 1998. Sequence-alignment modelling and molecular docking studies of the epoxygenase component of alkene monooxygenase from *Nocardia corallina* B-276. Eur. J. Biochem. 254, 480–489.

Gunsalus, I.C., Wagner, G.C., 1978. Bacterial P-450cam methylene monooxygenase components: cytochrome m, putidaredoxin, and putidaredoxin reductase. Methods Enzymol. 52, 166–188.

Harayama, S., Leppik, R.A., Rekik, M., Mermod, N., Lehrbach, P.R., Reineke, W., Timmis, K.N., 1986. Gene order of the TOL catabolic plasmid upper pathway operon and oxidation of both toluene and benzyl alcohol by the *xylA* product. J. Bacteriol. 167, 455–461.

Harayama, S., Rekik, M., Wubbolts, M., Rose, K., Leppik, R.A., Timmis, K.N., 1989. Characterization of five genes in the upper-pathway operon of TOL plasmid pWW0 from *Pseudomonas putida* and identification of the gene products. J. Bacteriol. 171, 5048–5055.

Harayama, S., Kok, M., Neidle, E.L., 1992. Functional and evolutionary relationships among diverse oxygenases. Annu. Rev. Microbiol. 46, 565–601.

Harder, J., Probian, C., 1995. Microbial degradation of monoterpenes in the absence of molecular oxygen. Appl. Environ. Microbiol. 61, 3804–3808.

Hopper, D.J., 1988. Properties of p-cresol methylhydroxylases. In: Hagedorn, S.R., Hansan, R.S., Kunz, D.A. (Eds.), Microbial Metabolism and the Carbon Cycle. Harwood Academic Publishers, Switzerland, pp. 247–258.

James, K.D., Williams, P.A., 1998. ntn genes determining the early steps in the divergent catabolism of 4-nitrotoluene and toluene in *Pseudomonas* sp. strain TW3. J. Bacteriol. 180, 2043–2049.

Kok, M., Oldenhuis, R., vander Linden, M.P.G., Raatjes, P., Kingma, J., van Lelyveld, P.H., Witholt, B., 1989. The *Pseudomonas oleovorans* alkane hydroxylase gene: sequence and expression. J. Biol. Chem. 262, 5435–5441.

Kovaleva, E.G., Lipscomb, J.D., 2008. Versatility of biological non-heme Fe (II) centers in oxygen activation reactions. Nat. Chem. Biol. 4, 186–193.

Lee, K., Ryu, E.K., Choi, K.S., Cho, M.C., Jeong, J.J., Choi, E.N., Lee, S.O., Yoon, D.Y., Hwang, I., Kim, C.K., 2006. Identification and expression of the cym, cmt, and tod catabolic genes from *Pseudomonas putida* KL47: expression of the regulatory todST genes as a factor for catabolic adaptation. J. Microbiol. 44, 192–199.

Madhyastha, K.M., Rangachari, P.N., Rao, M.R., Bhattacharyya, P.K., 1968. Microbiological transformations of terpenes. Part XV. Enzyme systems in the catabolism of *p*-cymene in PL-strain. Indian J. Biochem. 5, 167–173.

Nelson, D.R., 2006. Cytochrome P450 nomenclature, 2004. Methods Mol. Biol. 320, 1–10.

O'Connor, C.D., Humphries, G.O., 1982. Expression of the EcoR1 restriction-modification system and the construction of positive-selection cloning vectors. Gene 20, 219–229.

Panke, S., Witholt, B., Schmid, A., Wubbolts, M.G., 1998. Towards a biocatalyst for (S)-styrene oxide production: characterization of the styrene degradation pathway of *Pseudomonas* sp. strain VLB120. Appl. Environ. Microbiol. 64, 2032–2043.

Peix, A., Valverde, A., Rivas, R., Igual, J.M., Ramírez-Bahena, M.H., Mateos, P.F., Santa-Regina, I., Rodríguez-Barrueco, C., Martínez-Molina, E., Velázquez, E., 2007. Reclassification of *Pseudomonas aurantiaca* as a synonym of *Pseudomonas chlororaphis* and proposal of three subspecies, *P. chlororaphis* subsp. *chlororaphis* subsp. nov., *P. chlororaphis* subsp. *aureofaciens* subsp. nov., comb. nov. and *P. chlororaphis* subsp. *aurantiaca* subsp. nov., comb. Nov. Int. J. Syst. Evol. Microbiol. 57, 1286–1290.

Radke, M., 1987. Organic geochemistry of aromatic hydrocarbons. Adv. Petrol. Geochem. 2, 141–207.

Sanger, F., Nicklen, S., Coulson, A.R., 1977. DNA sequencing with chain-terminating inhibitors. Proc. Natl. Acad. Sci. USA 74, 5463–5467.

Schwartz, J.K., Wei, P.P., Mitchell, K.H., Fox, B.G., Solomon, E.I., 2008. Geometric and electronic structure studies of the binuclear nonheme ferrous active site of toluene-4-monooxygenase: parallels with methane monooxygenase and insight into the role of the effector proteins in O2 activation. J. Am. Chem. Soc. 130, 7098–7109.

Shanklin, J., Whittle, E., 2003. Evidence linking the *Pseudomonas oleovorans* alkane omega-hydroxylase, an integral membrane diiron enzyme, and the fatty acid desturase family. FEBS Lett. 545, 188–192.

Shanklin, J., Whittle, E., Fox, B.G., 1994. Eight histidine residues are catalytically essential in a membrane-associated iron enzyme, stearoyl-coenzyme A desaturase, and are conserved in alkane hydroxylase and xylene monooxygenase. Biochemistry 33, 12787–12794.

Shanklin, J., Achim, C., Schmidt, H., Fox, B.G., Munck, E., 1997. Mössbauer studies of alkane ω-hydroxylase: evidence for a diiron cluster in an integral-membrane enzyme. Proc. Natl. Acad. Sci. USA 94, 2981–2986.

Shanklin, J., Guy, J.E., Mishra, G., Lindqvist, Y., 2009. Desaturases: emerging models for understanding functional diversification of diiron-containing enzymes. J. Biol. Chem. 284, 18559–18563.

Shu, L., Nesheim, J.C., Kauffmann, K., Munck, E., Lipscomb, J.D., Que Jr., L., 1997. An $Fe_2^{IV}O_2$diamond core structure for the key intermediate Q of methane monooxygenase. Science 275, 515–518.

Singh, H.P., Kohli, R.K., Batish, D.R., Kaushal, P.S., 1999. Allelopathy of gymnospermous trees. J. Forest Res. 4, 245–254.

Suzuki, M., Hayakawa, T., Shaw, J.P., Rekik, M., Harayama, S., 1991. Primary structure of xylene monooxygenase: similarities to and differences from the alkane hydroxylation system. J. Bacteriol. 173, 1690–1695.

Thompson, J.D., Gilson, T.J., Plewniak, F., Jeanmougin, F., Higgins, D.G., 1997. The ClustalX windows interface: flexible strategies for multiple sequence alignment aided by quality analysis tools. Nucleic Acids Res. 24, 4876–4882.

Velasco, A., Alonso, S., Garcia, J.L., Perera, J., Diaz, E., 1998. Genetic and functional analysis of the styrene catabolic cluster of *Pseudomonas* sp. Strain Y2. J. Bacteriol. 180, 1063–1071.

Yanisch-Perron, C., Viera, J., Messing, J., 1985. Improved M13 phage cloning vectors and host strains: nucleotide sequences of the M13mp18 and pUC19 vectors. Gene 33, 103–119.